Influence of roughening transition on magnetic ordering

Nalina Vadakkayil,[1] Sanat K. Singha,[1,2] and Subir K. Das[1,*]

[1]*Theoretical Sciences Unit and School of Advanced Materials, Jawaharlal Nehru Centre for Advanced Scientific Research, Jakkur P.O., Bangalore 560064, India*

[2]*Assam Energy Institute, Centre of Rajiv Gandhi Institute of Petroleum Technology, Sivasagar 785697, India*

(Received 1 July 2021; revised 20 January 2022; accepted 31 March 2022; published 26 April 2022)

In the literature of magnetic phase transitions, in addition to a critical point, the existence of another special point has been discussed. This is related to the broadening of the interface between two different ordering phases and is referred to as the point of roughening transition. While the equilibrium properties associated with this transition are well understood, the influence of this on nonequilibrium dynamics still needs to be investigated. In this paper we present comprehensive results, from Monte Carlo simulations, on coarsening dynamics in a system, over a wide range of temperature, in space dimension $d = 3$, for which there exists a roughening transition at a nonzero temperature T_R. An advanced analysis of the simulation data, on structure, growth, and aging, shows that the onset of unexpected *glasslike* slow dynamics in this system, that has received attention in recent times, for quenches to zero temperature, actually occurs at this transition point. This implies that the structure and aging depend upon the final temperature, when the latter lies between 0 and T_R. This is a very interesting exception to universality in coarsening dynamics. The results also demonstrate an important structure-dynamics connection in the phase-ordering dynamics. We compare the key results with those from $d = 2$, for which there exists no nonzero roughening transition temperature. The absence of the above-mentioned anomalous features in the latter dimension places our conjecture on the role of the roughening transition on a firmer footing.

DOI: 10.1103/PhysRevE.105.044142

I. INTRODUCTION

Over the past several decades there has been significant interest [1–25] in the understanding of ordering dynamics following quenches of paramagnetic configurations to the ferromagnetic region by crossing the critical temperature [26] T_c. In recent times *glasslike* dynamics in a popular ordering system, viz., in the Ising model, following quenches to the final temperature $T_f = 0$, drew attention [6–8,10,11,13–17]. This is despite the absence of an in-built frustration in the above-mentioned model. This slow dynamics perhaps is due to a nonconventional structure formation. The observation is striking and it is unknown whether such unexpected behavior [9,15–17] is specific to $T_f = 0$. It is possible that the origin is at the roughening transition [27], that occurs at a much higher temperature T_R ($<T_c$), given that below T_R the interfaces are sharp. Knowledge of this is crucial not only in the understanding of this intriguing fact but also in establishing structure-dynamics coupling in the general context of growth phenomena. Interestingly, the consequences of the presence or absence of rough interfaces, of importance in real systems, in such nonequilibrium phenomena still needs to be investigated.

Some of the key aspects of ordering dynamics [23–25,28–38] are (i) self-similarity and the scaling property of the structure, (ii) growth of the latter, and (iii) related aging. The structure is typically probed via the two-point equal time (t) correlation function [28], which, for a spin system, reads $C(r,t) = \langle S_i(t)S_j(t)\rangle - \langle S_i(t)\rangle\langle S_j(t)\rangle$, with S_i and S_j representing the orientations of spins or atomic magnets at sites i and j, located r distance apart. It is also customary to study the Fourier transform of $C(r,t)$, the structure factor $S(k,t)$, with k being the wave number [28]. The latter has direct experimental relevance. These quantities obey certain scaling properties when the growth is self-similar. For example, in simple situations, when structures are nonfractal, $C(r,t)$ satisfies [28] $C(r,t) \equiv \tilde{C}(r/\ell)$, with ℓ being the average domain size or characteristic length scale of the growing system at time t and $\tilde{C}(x)$ a time-independent master function. In such a situation ℓ is expected [28] to grow as $\sim t^{\alpha}$. A power-law behavior is expected for the aging phenomena also. In the latter case the autocorrelation function [29,30], $C_{\rm ag}(t,t_w) = \langle S_i(t)S_i(t_w)\rangle - \langle S_i(t)\rangle\langle S_i(t_w)\rangle$, should scale as $\sim(\ell/\ell_w)^{-\lambda}$, in the asymptotic limit when $\ell \gg \ell_w$. Here, t_w ($\leqslant t$) is the waiting time or age of the system and ℓ_w is the value of ℓ at $t = t_w$.

For uniaxial ferromagnets one expects [28,37] $\alpha = 1/2$. The structure in this case is usually described by the Ohta-Jasnow-Kawasaki (OJK) function [24,28] $C(r,t) = \frac{2}{\pi}\sin^{-1}[\exp(-r^2/Dt)]$, with D being a constant. While the form of $C(r,t)$ and the value of the growth exponent α are independent of space dimension d, the aging exponent λ changes with the latter. The values of λ for this ordering, as obtained by Liu and Mazenko (LM) [23], are expected to be $\simeq 1.67 = \lambda_3^{\rm LM}$ in $d = 3$, whereas in $d = 2$ it is $\lambda_2^{\rm LM} \simeq 1.29$. Unless otherwise mentioned, in the rest of the paper all our discussions are for $d = 3$.

While these predictions were confirmed via Monte Carlo (MC) [38] simulations of the Ising model, for moderately high

*das@jncasr.ac.in

values of T_f, striking deviations were reported for $T_f = 0$, in $d = 3$. In this case, several works concluded that $\alpha = 1/3$ or the growth is even slower. Most recently it was reported that the OJK function does not [17] describe the pattern [39], i.e., the structure that is formed by domains rich in "up" and "down" spins, at $T_f = 0$. Furthermore, λ was also estimated [17] to be much weaker than $\lambda_3^{\rm LM}$. Thorough investigations, we believe, are necessary to arrive at a complete and correct picture. It needs to be understood if such anomalies bear any connection with any other special point. If such a special point turns out to be that of the roughening transition, an important relation concerning the structure and dynamics [40] can be established in the nonequilibrium context. Our MC study clearly suggests that the above-mentioned anomalous features are not specific to $T_f = 0$. The onset of the anomalies occurs at the roughening transition. Some key results have been verified by a sophisticated finite-size scaling analysis [34,41,42]. We believe that these will inspire further investigations, for reasons described later.

II. MODEL AND METHODS

We choose $J > 0$ in the Ising Hamiltonian [26,38] $H = -J \sum_{\langle ij \rangle} S_i S_j$, where S_i and S_j can take values $+1$ and -1, corresponding to up and down orientations of the atomic magnets. We study this model on a simple cubic lattice, having $T_c \simeq 4.51 J/k_B$ [38], where k_B is the Boltzmann constant. For the limited set of results in $d = 2$, we considered the square lattice. Note that in this case $T_c \simeq 2.27 J/k_B$ [38]. In $d = 3$, the value of T_R for this model is $\simeq 2.57 J/k_B$ [27], whereas a nonzero roughening transition temperature does not exist in $d = 2$. Moves in our MC simulations were tried by randomly choosing a spin and changing its sign [38,43]. These were accepted by following the standard Metropolis criterion [38]. The unit of time in our simulations is a MC step (MCS) that consists of L^d trial moves, with L being the linear dimension of a cubic or a square box, in units of the lattice constant.

All our results are presented after averaging over runs with 50 independent random initial configurations, with $L = 512$. A consideration of larger systems will keep the conclusions unchanged. However, with much larger systems, accessing very late-time dynamics will be difficult in $d = 3$. Periodic boundary conditions were applied in all possible directions. Average domain lengths were measured, from the simulation snapshots, as the first moments [36] of the domain-size distribution function, in which the length of a domain was estimated as the distance between two successive or consecutive interfaces along any Cartesian direction. Results on the structure and growth were obtained after appropriately eliminating the thermal noise in the snapshots via a majority-spin rule [36]. In this procedure a spin is provided with the sign of the majority of spins in its neighborhood, including itself. The noise removal was important for the analysis purpose, especially for very high temperatures ($T_f \gtrsim 2$). We repeat, unless otherwise stated, the results are from $d = 3$.

III. RESULTS

In Fig. 1 we show ℓ vs t plots for several values of T_f. The percentage errors, with respect to the mean values, in the data points lie in the range [0.03,2] in the finite-size "unaffected" regimes, being higher at later times. The latter is expected due to the decreasing number of domains with the increase of time. For $T_f = 0$ few early works [7,12–14] were suggestive of an exponent $\alpha = 1/3$ or even slower growth. Similar quantitative behavior is seen here as well. However, at a very late time a crossover [15,17] of the exponent to a higher value, viz., $\alpha = 1/2$, can be recognized. The very early works could not capture this, either due to the consideration of small systems or simulations over short periods, owing, perhaps, to inadequate computational resources. As can be seen, such a *slow looking* early growth is not unique to $T_f = 0$. The data sets for nonzero T_f values also exhibit a similar trend. However, with the increase of T_f the departure from this slow behavior occurs earlier, with the 1/3-like regime ceasing to exist for $T_f = T_R \simeq 2.57$. At this stage, it is worth warning that the early evolution should not be taken seriously, at the quantitative level. This is because, during this period satisfaction of the scaling property of the correlation function is not observed, as demonstrated below.

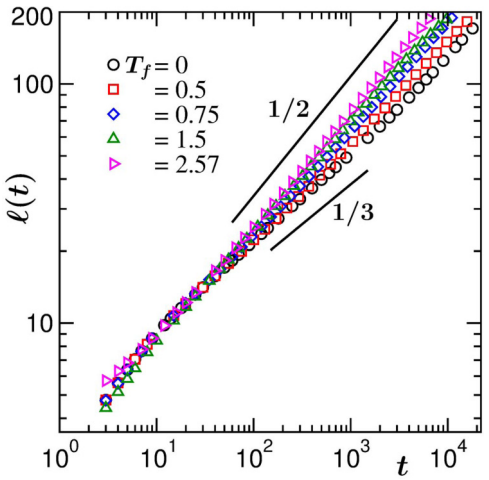

FIG. 1. Average domain lengths $\ell(t)$ are plotted vs time, on a log-log scale. Results from different final temperatures are presented. The solid lines are power laws. The values of the exponents are mentioned. Minor bendings in the long-time limit in some of the data sets are due to finite-size effects

In Fig. 2(a) we show plots of $C(r, t)$, from different times, by scaling the distance axis by a characteristic length, extracted by exploiting the satisfaction of scaling of $C(r, t)$ at small distances, for $T_f = 0.5$. The error bars here and for the autocorrelation functions are smaller than the symbol sizes. It appears that the collapse starts only from $t \gtrsim 1000$, approximately the time since the departure to $\alpha = 1/2$ behavior starts. This general picture is true for other low temperatures also. In Fig. 2(b) we have shown $C(r, t)$, again versus r/ℓ, from the scaling regimes of different T_f values. Interestingly, $\tilde{C}(r/\ell)$ at different T_f values do not agree with each other. However, with the increase of T_f the agreement with the OJK function [$\tilde{C}_{\rm OJK}(r/\ell)$] [24] keeps getting better. This observation suggests that perhaps there exists a special temperature $T_{\rm sp}$ ($< T_c$), beyond which the coarsening dynamics is more unique than below it. In fact, for $T_f = T_R$ the agreement between simulation data and the OJK function is quite well. We will

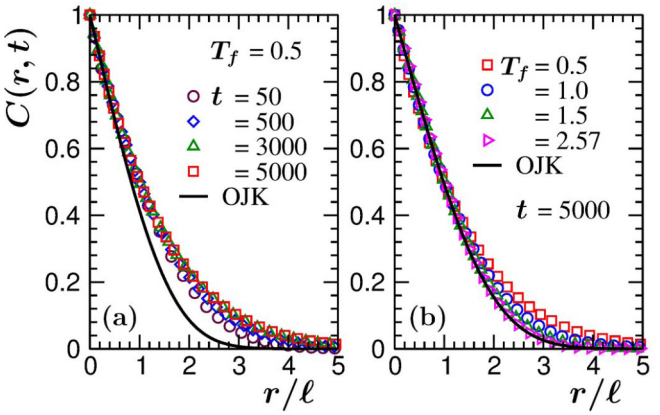

FIG. 2. (a) Two-point equal time correlation functions $C(r,t)$ are plotted vs the scaled distance r/ℓ, for $T_f = 0.5$. Data from a few different times are shown. (b) Same as (a) but here we have shown $C(r,t)$ from different final temperatures. In each of the cases we have chosen $t = 5000$ that fall in the scaling regimes. In both (a) and (b) the continuous lines represent the Ohta-Jasnow-Kawasaki (OJK) function. The correlation functions have been plotted in such a way that there exists good collapse in the early abscissa range.

return to this central theme after discussion of the basic results on aging. It will be seen that indeed $T_{\rm sp} = T_R$.

Figure 3(a) shows plots of $C_{\rm ag}(t,t_w)$, with a variation of ℓ/ℓ_w. The value of T_f for this representative case is 1.5. Data from a few different waiting times are shown. Good collapse is visible for the considered values of t_w. However, there exist deviations from the master curve, for $\ell/\ell_w \gg 1$. These are related to finite-size effects [34]. Decay in the finite-size unaffected regime is not consistent with the LM value [23]—see the disagreement with the solid line. In Fig. 3(b) we show the instantaneous exponent [30,34] $\lambda_i[= -d\ln C_{\rm ag}(t,t_w)/d\ln(\ell/\ell_w)]$ as a function of ℓ_w/ℓ, for multiple choices of t_w lying in the scaling regime. The data sets appear linear in the finite-size unaffected regimes. Note that at the early time relaxation of domain magnetization interferes and should be discarded from the process of estimating λ. A linear extrapolation to $\ell/\ell_w = \infty$ asymptotically provides $\lambda \simeq 1.5$. Given that the above quoted number lies between $\lambda_3^{\rm LM}$ and $\lambda(T_f = 0)$, which is significantly different from each of these, one gets a strong indication of the presence of a special point.

In Fig. 3(c) we show plots of λ_i vs ℓ_w/ℓ, for a few different values of T_f. Here, we discarded the parts corresponding to finite-size effects and the equilibration of domain magnetization. Furthermore, in each of the cases the results are from well inside the scaling regimes of t_w. The arrowheaded lines are related to the estimations of the values of λ, from linear extrapolations to the asymptotic limit $\ell/\ell_w = \infty$. Clearly, λ depends strongly on T_f. The accuracy of these estimates is validated by the independent quantifications of λ via a finite-size scaling method [34,42]. A representative exercise related to this is shown in Fig. 3(d), for $T_f = 0.75$. In this figure Y is a t_w-independent scaling function and y is a dimensionless scaling variable. Here, we have avoided studying systems of different sizes, contrary to the standard practice in the literature of such an analysis. Instead, we have obtained a

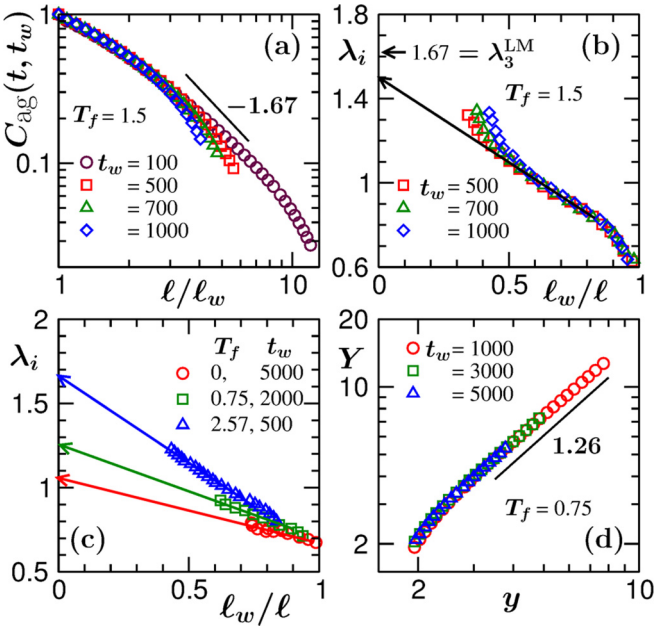

FIG. 3. (a) $C_{\rm ag}(t,t_w)$, the autocorrelation functions, are plotted vs ℓ/ℓ_w, on a log-log scale. Data from different t_w, for $T_f = 1.5$, are included. The solid line is a power law with $\lambda = \lambda_3^{\rm LM} = 1.67$. (b) The instantaneous exponents λ_i are shown as a function of ℓ_w/ℓ, for the same final temperature. The arrowheaded line is a linear extrapolation to the $\ell/\ell_w = \infty$ limit, done by excluding the late time finite size affected as well as early-time domain-magnetization relaxation parts. (c) Here, we have shown λ_i, as a function of ℓ_w/ℓ, for a few different values of T_f. In each of the cases t_w belongs to the scaling regime. The arrowheaded lines are linear guides to the eyes. (d) Finite-size scaling plot of $C_{\rm ag}(t,t_w)$ for $T_f = 0.75$. The solid line there corresponds to a power law with the value of the exponent mentioned near the line.

collapse of data from different t_w values. When t_w is varied, a system has different effective sizes to grow further, fulfilling the requirement of different system sizes. See below for the details on the scaling method. The behavior of λ_i in Figs. 3(b) and 3(c) suggests $\lambda_i = \lambda - B/x$, with $x = \ell/\ell_w$ and B being a

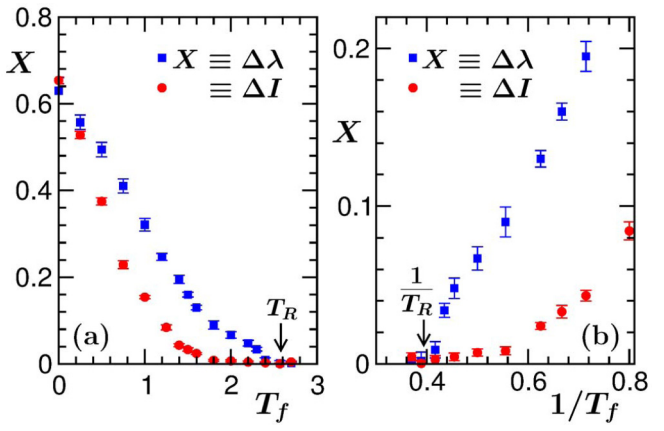

FIG. 4. (a) Plots are shown by comparing $\Delta\lambda$ and ΔI with the variation of T_f. (b) Plots of $\Delta\lambda$ and ΔI as a function of $1/T_f$. The locations of T_R are marked inside the frames.

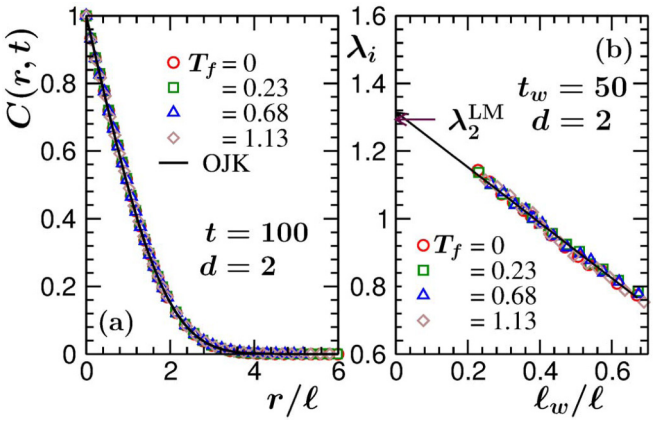

FIG. 5. (a) Plots of scaled two-point equal time correlation functions $C(r,t)$, from $d=2$, for different T_f values. The time has been chosen from the scaling regime. The continuous line represents the OJK function. (b) The instantaneous exponents λ_i are plotted as a function of ℓ_w/ℓ, for different T_f values. The solid line is a common linear extrapolation of the data sets. The arrowheaded horizontal line points to the LM value of λ in $d=2$.

constant, in the finite-size unaffected late-time regime. This leads to a form [34,42] $C_{\rm ag}(t,t_w) = Ae^{-B/x}x^{-\lambda}$. By taking $y = L/\ell$ as a scaling variable and $y_w = L/\ell_w$, a finite-size scaling function can be written as [17] $Y = C_{\rm ag}(t,t_w)e^{By/y_w}y_w^{\lambda}$, where Y contains a factor y^{λ}. When results from different t_w are plotted, for optimum choices of the unknown parameters, including λ, there will be a collapse of data sets that will satisfy the expected y^{λ} behavior at large y. This is demonstrated in Fig. 3(d) for $T_f = 0.75$. Here, the collapse is obtained for $\lambda = 1.26$, the number being consistent with the value that was suggested by the exercise in Fig. 3(c). Next, we quantify the special temperature from a more systematic study.

In Fig. 4(a) we show $\Delta\lambda = \lambda_3^{\rm LM} - \lambda(T_f)$, as a function of T_f. Given that the earlier temperature-independent expectation is $\lambda_3^{\rm LM}$, it is meaningful to look at the stated difference. There appears to be a nice convergence of the data set to zero as $T_f \to T_{\rm R} \simeq 2.57$. With respect to the deviation of $\tilde{C}(r/\ell)$ from the OJK form [24], that we observed above, there may also be a similar trend. In this case an appropriate quantity to consider is $\Delta I = \int dr[\tilde{C}(r/\ell) - \tilde{C}_{\rm OJK}(r/\ell)]$. Here, note that there exists an LM form for $C(r,t)$ as well [23]. However, this practically overlaps with the OJK function. It will be interesting to see if ΔI approaches zero at the same T_f as in the case of $\Delta\lambda$. Thus, in Fig. 4(a) we have included the T_f dependence of ΔI as well. The trends in the presented data sets are in nice agreement with each other, over a wide range of temperature—see Fig. 4(b) for clearer convergences of $\Delta\lambda$ and ΔI to zero for $T_f \to T_R$.

Figure 5 contains analogous results from $d=2$. In Fig. 5(a) we show the scaled $C(r,t)$ and Fig. 5(b) shows data for λ_i vs ℓ_w/ℓ. For each of the cases results from a wide range of T_f are included. The anomalies present in $d=3$ are clearly absent in this case. No detectable T_f dependence can be observed. The theoretical expectations are satisfied over the whole range of T_f. Recall that in this dimension, a nonzero roughening transition temperature does not exist for this model.

IV. CONCLUSION

From extensive simulations [38] we have presented results on nonequilibrium dynamics in the Glauber [38,43] Ising model. This mimics ordering in uniaxial ferromagnets. Our quantitative analysis of data from space dimension $d=3$ on the structure, growth, and aging, over a wide range of temperature below the critical point, suggests that the low-temperature behavior is anomalous. We show that the anomalies are not unique to the case of zero-temperature quench, as was previously thought. Various quantities exhibit a zero-temperature-like trend until a certain nonzero value of T_f. Above this temperature, the behavior of all the aspects becomes consistent with various theoretical expectations [23,24,28,37]. This *transition or special temperature* coincides with that of the roughening transition [27]. Such a conclusion appears more meaningful from the fact that this interesting nonuniversality is absent in $d=2$ and for this dimension the roughening transition temperature is zero.

To understand this exceptional behavior more detailed theoretical investigations by exploiting the well-traveled auxiliary field ansatz should be carried out [44]. Recently, it was shown [45] that the ordering dynamics in the Glauber Ising model exhibits the Mpemba effect (ME). Considering the surprising observation here and the discovery of ME in the same model, it will be interesting to see how in $d=3$ the interplay between initial correlation and the final temperature brings out further different features. The structure-dynamics connection shown here can be of importance in the domains of other passive [46–51] as well as active matter systems [52], where interface roughness is of interest.

ACKNOWLEDGMENTS

The authors are grateful to SERB, DST, India for support via Grant No. MTR/2019/001585. They also acknowledge computation times at computer clusters of National Supercomputing Mission located at JNCASR.

[1] V. Spirin, P. L. Krapivsky, and S. Redner, Phys. Rev. E **63**, 036118 (2001).
[2] V. Spirin, P. L. Krapivsky, and S. Redner, Phys. Rev. E **65**, 016119 (2001).
[3] P. M. C. de Oliveira, C. M. Newman, V. Sidoravicious, and D. L. Stein, J. Phys. A: Math. Gen. **39**, 6841 (2006).
[4] G. Kondrat and K. Sznajd-Weron, Phys. Rev. E **79**, 011119 (2009).

[5] J. J. Arenzon, A. J. Bray, L. F. Cugliandolo, and A. Sicilia, Phys. Rev. Lett. **98**, 145701 (2007).

[6] J. Olejarz, P. L. Krapivsky, and S. Redner, Phys. Rev. Lett. **109**, 195702 (2012).

[7] J. Olejarz, P. L. Krapivsky, and S. Redner, Phys. Rev. E **83**, 051104 (2011).

[8] J. Olejarz, P. L. Krapivsky, and S. Redner, Phys. Rev. E **83**, 030104 (2011).

[9] F. Corberi, E. Lippiello, and M. Zannetti, Phys. Rev. E **78**, 011109 (2008).

[10] T. Blanchard, F. Corberi, L. F. Cugliandolo, and M. Picco, Europhys. Lett. **106**, 66001 (2014).

[11] T. Blanchard, L. F. Cugliandolo, M. Picco, and A. Tartaglia, J. Stat. Mech. (2017) 113201.

[12] A. Lipowski, Physica A **268**, 6 (1999).

[13] J. D. Shore, M. Holzer, and J. P. Sethna, Phys. Rev. B **46**, 11376 (1992).

[14] S. Cueille and C. Sire, J. Phys. A: Math. Gen. **30**, L791 (1997).

[15] S. K. Das and S. Chakraborty, Eur. Phys. J.: Spec. Top. **226**, 765 (2017).

[16] S. Chakraborty and S. K. Das, Europhys. Lett. **119**, 50005 (2017).

[17] N. Vadakkayil, S. Chakraborty, and S. K. Das, J. Chem. Phys. **150**, 054702 (2019).

[18] J. Denholm and B. Hourahina, J. Stat. Mech. (2020) 093205.

[19] C. Godrèche and M. Pleimling, J. Stat. Mech. (2018) 043209.

[20] P. Mullick and P. Sen, Phys. Rev. E **95**, 052150 (2017).

[21] U. Yu, J. Stat. Mech. (2017) 123203.

[22] L. F. Cugliandolo, C. R. Phys. **16**, 257 (2015).

[23] F. Liu and G. F. Mazenko, Phys. Rev. B **44**, 9185 (1991).

[24] T. Ohta, D. Jasnow, and K. Kawasaki, Phys. Rev. Lett. **49**, 1223 (1982).

[25] C. Yeung, Phys. Rev. Lett. **61**, 1135 (1988).

[26] M. E. Fisher, Rep. Prog. Phys. **30**, 615 (1967).

[27] H. van Beijern and I. Nolden, in *Structure and Dynamics of Surfaces II: Phenomena, Models and Methods*, edited by W. Schommers and P. von Blanckenhagen, Topics in Current Physics (Springer, Berlin, 1987), Vol. 43.

[28] A. J. Bray, Adv. Phys. **51**, 481 (2002).

[29] *Kinetics of Phase Transitions*, edited by S. Puri and V. Wadhawan (CRC Press, Boca Raton, FL, 2009).

[30] D. S. Fisher and D. A. Huse, Phys. Rev. B **38**, 373 (1988).

[31] C. Yeung, M. Rao, and R. C. Desai, Phys. Rev. E **53**, 3073 (1996).

[32] M. Henkel, A. Picone, and M. Pleimling, Europhys. Lett. **68**, 191 (2004).

[33] E. Lorenz and W. Janke, Europhys. Lett. **77**, 10003 (2007).

[34] J. Midya, S. Majumder, and S. K. Das, J. Phys.: Condens. Matter **26**, 452202 (2014).

[35] D. A. Huse, Phys. Rev. B **34**, 7845 (1986).

[36] S. Majumder and S. K. Das, Phys. Rev. E **84**, 021110 (2011).

[37] S. M. Allen and J. W. Cahn, Acta Metall. **27**, 1085 (1979).

[38] D. P. Landau and K. Binder, *A Guide to Monte Carlo Simulations in Statistical Physics* (Cambridge University Press, Cambridge, UK, 2009).

[39] M. C. Cross and P. C. Hohenberg, Rev. Mod. Phys. **65**, 851 (1993).

[40] J. Midya and S. K. Das, Phys. Rev. Lett. **118**, 165701 (2017).

[41] M. E. Fisher and M. N. Barber, Phys. Rev. Lett. **28**, 1516 (1972).

[42] J. Midya, S. Majumder, and S. K. Das, Phys. Rev. E **92**, 022124 (2015).

[43] R. J. Glauber, J. Math. Phys. **4**, 294 (1963).

[44] C. Yeung, Phys. Rev. E **97**, 062107 (2018).

[45] N. Vadakkayil and S. K. Das, Phys. Chem. Chem. Phys. **23**, 11186 (2021).

[46] J. P. van der Eerden, J. Cryst. Growth **128**, 62 (1993).

[47] X.-Y. Liu, P. Bennema, and J. P. van der Eerden, Nature (London) **356**, 778 (1992).

[48] T. H. Zhang and X.-Y. Liu, Chem. Soc. Rev. **43**, 2324 (2014).

[49] V. N. Gorshkov, V. V. Tereshchuk, and P. Sareh, CrystEngComm. **23**, 1836 (2021).

[50] I. Utke, C. Klemenz, H. J. Scheel, M. Sasaura, and S. Miyazawa, J. Cryst. Growth **174**, 806 (1997).

[51] A. Senyshyn, H. Ehrenberg, L. Vasylechko, J. D. Gale, and U. Bismayer, J. Phys.: Condens. Matter **17**, 6217 (2005).

[52] B. Trefz, S. K. Das, S. A. Egorov, P. Virnau, and K. Binder, J. Chem. Phys. **144**, 144902 (2016).